

Versatile Benzimidazole/Triphenylamine Hybrids: Efficient Nondoped Deep-Blue Electroluminescence and Good Host Materials for Phosphorescent Emitters

Shaolong Gong,^[a] Yongbiao Zhao,^[b] Meng Wang,^[a] Chuluo Yang,^{*[a]} Cheng Zhong,^[a] Jingui Qin,^[a] and Dongge Ma^{*[b]}

Abstract: Two new bipolar compounds, *N,N,N,N'*-tetraphenyl-5'-(1-phenyl-1*H*-benzimidazol-2-yl)-1,1':3',1''-terphenyl-4,4''-diamine (**1**) and *N,N,N,N'*-tetraphenyl-5'-(1-phenyl-1*H*-benzimidazol-2-yl)-1,1':3',1''-terphenyl-3,3''-diamine (**2**), were synthesized and characterized, and their thermal, photophysical, and electrochemical properties were investigated. Compounds **1** and **2** possess good thermal stability with high glass-transition temperatures of 109–129 °C and thermal decomposition temperatures of 501–531 °C. The fluorescence quantum yield of **1** (0.52) is higher than that of **2** (0.16), which could be attributed to greater π conjugation be-

tween the donor and acceptor moieties. A nondoped deep-blue fluorescent organic light-emitting diode (OLED) using **1** as the blue emitter displays high performance, with a maximum current efficiency of 2.2 cdA⁻¹ and a maximum external efficiency of 2.9% at the CIE coordinates of (0.17, 0.07) that are very close to the National Television System Committee's blue standard (0.15, 0.07). Electrophosphorescent devices using the two compounds

as host materials for green and red phosphor emitters show high efficiencies. The best performance of a green phosphorescent device was achieved using **2** as the host, with a maximum current efficiency of 64.3 cdA⁻¹ and a maximum power efficiency of 68.3 lmW⁻¹; whereas the best performance of a red phosphorescent device was achieved using **1** as the host, with a maximum current efficiency of 11.5 cdA⁻¹, and a maximum power efficiency of 9.8 lmW⁻¹. The relationship between the molecular structures and optoelectronic properties are discussed.

Keywords: benzimidazole • host-guest systems • materials science • phosphorescence • triphenylamine

Introduction

As compared with the superior device performances of green and red emitters, blue-light-emitting materials and devices still need to be improved in terms of efficiency and color purity. Highly efficient blue organic light-emitting diodes (OLEDs) are a pressing concern for high-resolution full-color displays and solid-state lighting applications.^[1] Fur-

thermore, the development of a deep-blue emission, which is defined as having a Commission Internationale de L'Eclairage (CIE) *y* coordinate value of less than 0.15,^[2] is of special significance because such an emitter can not only effectively reduce the power consumption of a full-color OLED but also be utilized to generate light of other colors by energy cascade to a lower-energy fluorescent or phosphorescent dopant.^[3,4] Although the dopant system as an emitting layer has been proven to improve the device performance,^[3,5] the fabrication process became complicated and expensive during the mass production of OLEDs,^[5a] and therefore, the use of a nondoped emitting layer is of practical significance. Charge transporting and charge balancing are two crucial factors for high-efficiency OLEDs. To balance the electron-hole recombination, one promising strategy is to incorporate an electron-donating moiety and an electron-withdrawing moiety into a single emitter;^[4,6] however, this donor-acceptor system could cause a remarkable bathochromic effect, and thereby the color purity of the

[a] S. Gong, M. Wang, Prof. C. Yang, C. Zhong, Prof. J. Qin
Department of Chemistry
Hubei Key Lab on Organic and Polymeric Optoelectronic Materials
Wuhan University
Fax: (+86)276-875-6757
E-mail: clyang@whu.edu.cn

[b] Y. Zhao, Prof. D. Ma
State Key Laboratory of Polymer Physics and Chemistry
Changchun Institute of Applied Chemistry
Chinese Academy of Sciences, Changchun 130022 (P. R. China)
E-mail: mdg1014@ciac.jl.cn

blue emission might be impaired. To date, deep-blue light-emitting materials with bipolar transporting properties remain a great challenge.

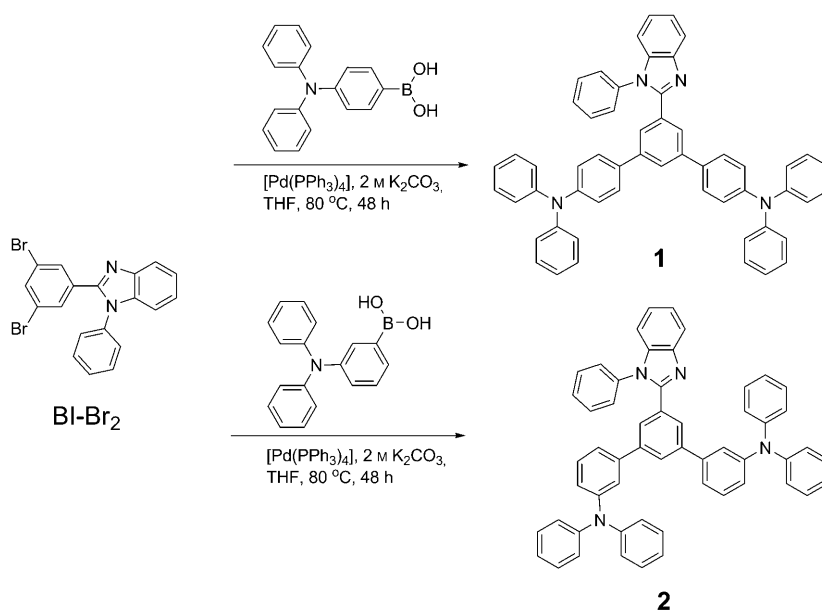
Over the past decade, considerable progress has been made in phosphorescent organic light-emitting diodes (PHOLEDs).^[7–10] For PHOLEDs, the phosphorescent dopant of a heavy metal complex has to be doped in the host materials to reduce concentration quenching and triplet–triplet annihilation.^[11] Because of the intrinsically wide band gap of blue emitters, they could be utilized as host materials for phosphorescent emitters.

In our previous work, we reported two simple triphenylamine/oxadiazole derivatives as highly efficient blue emitters and hosts for red PHOLEDs and we realized two-color-based white OLEDs.^[12] However, the CIE coordinates of $y > 0.15$ for the new blue emitters were not satisfied. Herein, we report the design and synthesis of two new benzimidazole/triphenylamine hybrids through the Suzuki cross-coupling reaction. The benzimidazole unit was introduced as an electron-accepting component owing to its good electron mobility.^[4,13] Combined with the good hole mobility of arylamines,^[14] we decided to link the benzimidazole unit and the diphenylamine unit with an *m*-terphenyl spacer. We anticipate that the combination of benzimidazole and diphenylamine by means of the rigid *m*-terphenyl linkage can alleviate the intramolecular charge transfer from the donor to the acceptor, and this would therefore not only have little effect on the color purity of the blue-emissive materials with bipolar character, but would also avoid lowering the triplet energies of the hybrids to some extent. The proper triplet energies of the hybrids would ensure that they could host a phosphorescent emitter. A device that incorporates **1** as the emitter exhibits a maximum current efficiency of 2.2 cd A^{-1} , a maximum external efficiency of 2.9%, together with satisfactory CIE coordinates (0.17, 0.07). When **1** and **2** were used as host materials doped with phosphorescent emitters, efficient green and red PHOLEDs were obtained, respectively. Additionally, some relationship between the molecular structures and optoelectronic properties will be addressed in this paper.

Results and Discussion

Synthesis and Characterization

The new compounds, *N,N,N',N'*-tetraphenyl-5'-(1-phenyl-1*H*-benzimidazol-2-yl)-1,1':3',1''-terphenyl-4,4''-diamine (**1**) and *N,N,N',N'*-tetraphenyl-5'-(1-phenyl-1*H*-benzimidazol-2-yl)-1,1':3',1''-terphenyl-3,3''-diamine (**2**), were synthesized through Suzuki cross-coupling reactions of 2-(3,5-dibromophenyl)-1-phenyl-1*H*-benzimidazole (BI-Br₂) with 4-(diphenylamino)phenylboronic acid and 3-(diphenylamino)phenylboronic acid, respectively (Scheme 1).^[15] Their structures were fully characterized by ¹H and ¹³C NMR spectroscopy, mass spectrometry, and elemental analysis (see the Experimental Section).



Scheme 1. Synthesis and molecular structures of **1** and **2**.

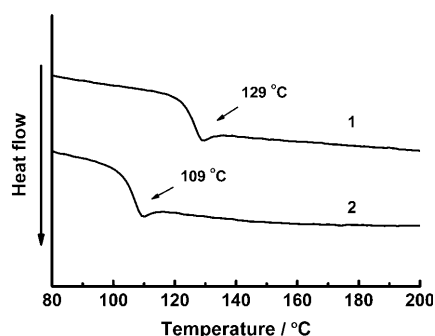
Thermal Properties

The thermal properties of the compounds were characterized using thermogravimetric analysis (TGA) and differential scanning calorimetry (DSC; Table 1). TGA measurements reveal their high thermal-decomposition temperatures (T_d , which corresponds to 5% weight loss) of 531 (**1**) and 501 °C (**2**). The DSC trace exhibits distinct glass-transition temperatures (T_g) of 129 (**1**) and 109 °C (**2**) during the second heating scans (Figure 1). Compound **2**, with a *meta* disposition between 1,2-diphenyl-1*H*-benzimidazole and the diphenylamine units, has a lower T_g value than **1** with a *para* disposition, which can be attributed to the greater energetic disorder in the *meta* derivatives.^[16] The high T_d and T_g values suggest that they could form morphologically stable and uniform amorphous films upon thermal evaporation, which is highly important to improve the efficiency and lifetime of OLEDs.

Table 1. Physical properties of **1** and **2**.

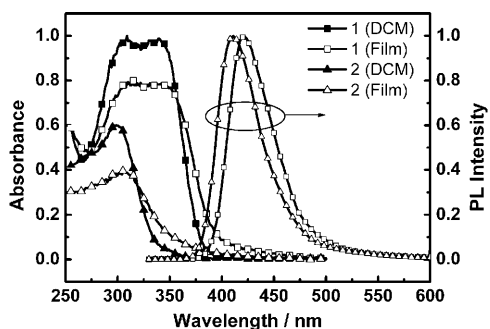
	1	2
$T_g/T_m/T_d$ [°C]	129/257/531	109/212/501
$\lambda_{\text{abs}}^{[a]}$ [nm]	309, 340	298
$\lambda_{\text{em,max}}^{[b]}$ [nm]	421	411
$\Phi^{[c]}$ [%]	52	16
HOMO/LUMO ^[d] [eV] _{exptl}	5.20/2.06	5.27/1.82
HOMO/LUMO ^[e] [eV] _{calcd}	5.22/1.48	5.28/1.50
$E_T^{[f]}$ [eV] _{exptl}	2.41	2.55
$\Delta E (T_1-S_0)^{[f]}$ [eV] _{calcd}	2.69	2.87

[a] Measured in dichloromethane. [b] Measured in the film state. [c] Measured in dichloromethane with an integrating sphere. [d] Determined from cyclic voltammetry and the absorption onset. [e] Obtained from DFT calculations. [f] Measured in the film state at 77 K.

Figure 1. DSC traces of **1** and **2** recorded at a heating rate of 10°Cmin⁻¹.

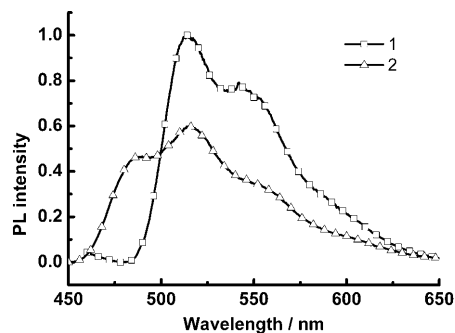
Photophysical Properties

The photophysical properties of the compounds were investigated by obtaining the UV/Vis absorption and photoluminescence (PL) spectra (Figure 2 and Table 1). The absorption bands around 300 nm for both **1** and **2** could be assigned to the triphenylamine-centered $n-\pi^*$ transition. The longer wavelength absorption band around 340 nm for **1** could be attributed to the charge transfer (CT) $\pi-\pi^*$ transition from the electron-donating triphenylamine moiety to the electron-accepting benzimidazole moiety. It is worth noting that the intramolecular charge-transfer transition for

Figure 2. UV/Vis absorption of **1** and **2** in dichloromethane or films, and PL spectra of **1** and **2** in films.

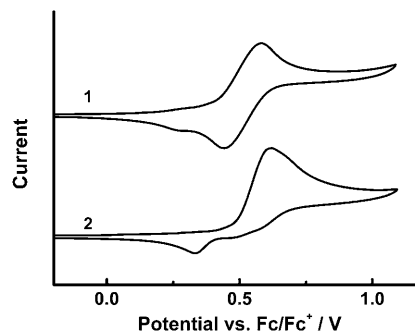
2 is almost completely suppressed owing to the minimizing conjugation between the donor and acceptor. For the same reason, the PL emission maximum of **2** (411 nm) is blue-shifted by 10 nm with respect to that of **1** (421 nm). The fluorescence quantum yield of **1** in dichloromethane (0.52) is substantially higher than that of **2** (0.16). This is attributed to the extended π conjugation for *para*-triphenylamine linked **1**. The high quantum yield of **1** also makes it a candidate for an efficient blue-light-emitting material in OLEDs.

To be an appropriate host material, the host should have higher triplet energy (E_T) than the phosphorescent guest emitter to prevent reverse energy transfer from the guest back to the host. The triplet energies (E_T) of **1** and **2**, determined by the highest-energy vibronic sub-band of the phosphorescence spectra in the film state at 77 K (Figure 3), are 2.41 and 2.55 eV, respectively; these values are high enough to host green or red phosphorescent emitters. Additionally, the triplet energy of **2** is significantly higher than that of **1**, which is associated with the decrease of π conjugation in the *meta* configuration.

Figure 3. Phosphorescence spectrum of **1** and **2** in the film state at 77 K.

Electrochemical Properties

Cyclic voltammetry (CV) was performed to investigate the electrochemical properties of the compounds. As shown in Figure 4, **1** and **2** exhibit one quasi-reversible, one-electron oxidation process, which can be assigned to the oxidation of the arylamine moiety. The HOMO energy levels of the com-

Figure 4. Cyclic voltammograms of **1** and **2** in CH₂Cl₂ for an oxidation scan.

pounds were determined from the onset of the oxidation potentials with regard to the energy level of ferrocene (4.8 eV below vacuum). The estimated HOMO levels are 5.20 (**1**) and 5.27 eV (**2**), which are similar to most triphenylamine derivatives. In CH_2Cl_2 , no reduction waves were detected for the two compounds owing to the benzimidazole structure.^[4] The LUMO energy levels were deduced from HOMO energy levels and energy gaps determined by the onset of absorption (Table 1). The deduced LUMO levels are 2.06 (**1**) and 1.82 eV (**2**).

Theoretical Calculations

To understand the structure–property relationship of the compounds at the molecular level, the geometric and electronic properties of the compounds were studied by density functional theory (DFT) and time-dependent DFT (TD-DFT) calculations using B3LYP hybrid functional (for details, see the Experimental Section). According to DFT calculations (Figure 5), the HOMO orbitals are mainly located

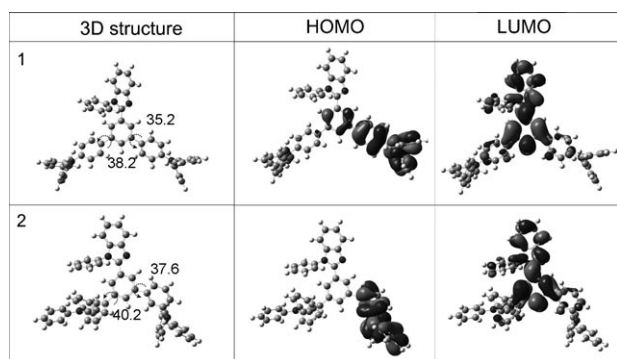


Figure 5. Optimized geometry and spatial distributions of the HOMO and LUMO levels of **1** and **2**.

on the electron-donating triphenylamine moiety, whereas the LUMO orbitals are mainly distributed on the electron-accepting benzimidazole moiety. Compounds **1** and **2** have almost complete separation of the HOMO and LUMO at the hole- and electron-transporting moieties, respectively, which most likely arise from the weak intramolecular charge transfer from the triphenylamine to the benzimidazole unit. Since the separation between HOMO and LUMO levels is preferable for efficient hole- and electron-transporting properties and the prevention of reverse energy transfer,^[17] **1** and **2** could be suitable as host materials for green or red phosphorescent emitters. The calculated triplet energy gaps $\Delta E (T_1-S_0)$ are 2.69 eV for **1** and 2.87 eV for **2**, which are in good agreement with the experimental results (Table 1). As shown in Figure 5, the optimized dihedral angles at the *m*-terphenyl spacer increase from 38.2 and 35.2° (**1**) to 40.2 and 37.6° (**2**), which suggests a decrease in the coupling between the electron donor and acceptor for **2**.

Electroluminescent Devices

To evaluate the applicability of **1** as the blue-emitting material, we fabricated nondoped blue-emitting device **A** with the configuration: ITO/MoO₃ (10 nm)/1,4-bis[(1-naphthylphenyl)amino]biphenyl (NPB, 80 nm)/**1** (20 nm)/1,3,5-tris(*N*-phenylbenzimidazol-2-yl)benzene (TPBI, 40 nm)/LiF (1 nm)/Al (100 nm). MoO₃ is used to promote hole injection and NPB serves as the hole-transporting material; TPBI and LiF act as the electron-transporting and electron-injecting layer, respectively. Device **A** exhibits deep-blue emission that peaks around 428 nm, with a narrow FWHM (full-width at half-maximum) of 51 nm at 7 V (Figure 6). It is noteworthy that the CIE chromaticity coordinates of (0.17, 0.07) are very close to the standard blue emission recommended by the National Television System Committee (NTSC, 0.15, 0.07)^[18] (inset of Figure 6).

Figure 7 shows current density–voltage–brightness (*J*–*V*–*L*) characteristics, and the current efficiency versus current density curve for device **A**. Device **A** displays satisfactory

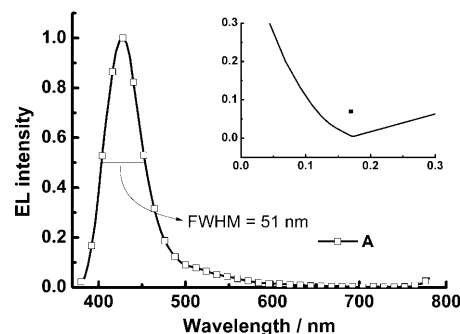


Figure 6. EL spectrum of device **A** operated at 7 V. Inset: CIE coordinates of device **A**.

device performance, with a maximum current efficiency ($\eta_{c,max}$) of 2.2 cd A^{-1} , a maximum power efficiency ($\eta_{p,max}$) of 1.6 lm W^{-1} , and a maximum external efficiency ($\eta_{ext,max}$) of 2.9%, which are comparable with the best device performance in the literature for the nondoped deep-blue OLEDs with a CIE coordinate of $y < 0.10$.^[19,20] For example, we recently reported a series of fluorine-based oligomers with spi-

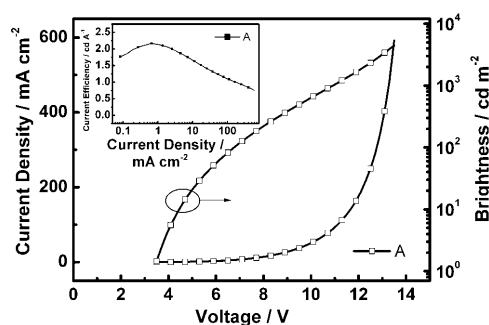


Figure 7. Current density–voltage–brightness characteristics of device **A**. Inset: Current efficiency versus current density curve for device **A**.

roannulated triarylamine as stable deep-blue emitters, and a maximum current efficiency of 1.91 cd A^{-1} at the CIE coordinates of (0.16, 0.07) was achieved.^[19c] Chien et al. reported a high-efficiency deep-blue OLED with a maximum current efficiency of 2.9 cd A^{-1} at the CIE coordinates of (0.15, 0.07) by utilizing a bipolar compound as the emitter.^[20c]

To investigate the utility of the two compounds as bipolar host materials for phosphors, we first fabricated green phosphorescent devices **B** and **C** by using **1** and **2** as hosts for green phosphorescent emitter $[\text{Ir}(\text{ppy})_3]$ ($\text{ppy} = 2\text{-phenylpyridine}$), respectively. The configurations of the devices are as follows: ITO/MoO₃ (10 nm)/NPB (80 nm)/**1** or **2**: 9 wt % $[\text{Ir}(\text{ppy})_3]$ (20 nm)/TPBI (40 nm)/LiF (1 nm)/Al (100 nm). The current density–voltage–brightness (J–V–L) characteristics, and the efficiency versus current density curves of the devices are shown in Figure 8. Electroluminescence (EL) data of the devices are summarized in Table 2. Devices **B** and **C** show typical green emission around 530 nm that originates from the guest $[\text{Ir}(\text{ppy})_3]$ (Figure 8d). Device **B** hosted by *para*-linked **1** shows a maximum luminance of 48428 cd m^{-2} at 11.9 V, a maximum current efficiency of 59.0 cd A^{-1} , and a maximum power efficiency of 48.7 lm W^{-1} . Better EL performance is achieved in device **C** hosted by *meta*-linked **2** (40702 cd m^{-2} at 10.9 V, 64.3 cd A^{-1} , and 68.3 lm W^{-1}). The triplet energy of **2** (2.55 eV) is higher than that of the guest $[\text{Ir}(\text{ppy})_3]$ (2.42 eV),^[21] whereas the triplet energy gap of **1** (2.41 eV) is close to that of $[\text{Ir}(\text{ppy})_3]$. The close triplet energies between the host and guest could allow for reverse energy transfer from the guest back to the host, and consequently decrease the efficiency of the device.

Finally, we also fabricated red phosphorescent devices **D** and **E** by doping **1** or **2** with 6 wt % bis(1-phenylisoquinolino-*N,C2'*)iridium(acetylacetonate) ($[(\text{piq})_2\text{Ir}(\text{acac})]$) ($E_T = 2.0 \text{ eV}$)^[22] in the same device structures as devices **B** and **C**. Devices **D** and **E** emit deep red light with CIE chromaticity coordinates of (0.68, 0.32). Device **E** hosted by **2** shows a maximum luminance of 11446 cd m^{-2} at 12.7 V, a maximum current efficiency of 6.5 cd A^{-1} , and a maximum power efficiency of 5.1 lm W^{-1} ; whereas device **D** hosted by **1** exhibits much better EL performance (23616 cd m^{-2} at 13.7 V, 11.5 cd A^{-1} , and 9.8 lm W^{-1}). Why does the device hosted by **1** display better red phosphorescent device performance than the device hosted by **2**? Conversely, why does the device hosted by **2** display better green phosphorescent device performance than the device hosted by **1**? This could be elucidated as follows: 1) for the green phosphorescent device, the discrepancy of triplet energy between the host and guest is the main factor affecting the device efficiency; and 2) for the red phosphorescent device, both **1** and **2** have a high enough triplet energy to host a red phosphor guest, and therefore the triplet energy of host does not determine the device efficiency. In this situation, the charge-transport ability of the host may become important for the device efficiency, and as a consequence, the lower charge-transport ability of **2** that owes itself to the *meta*-linkage may result in the inferior red-phosphorescent device efficiency. We note that all the phosphorescent devices (**B–E**) display low turn-

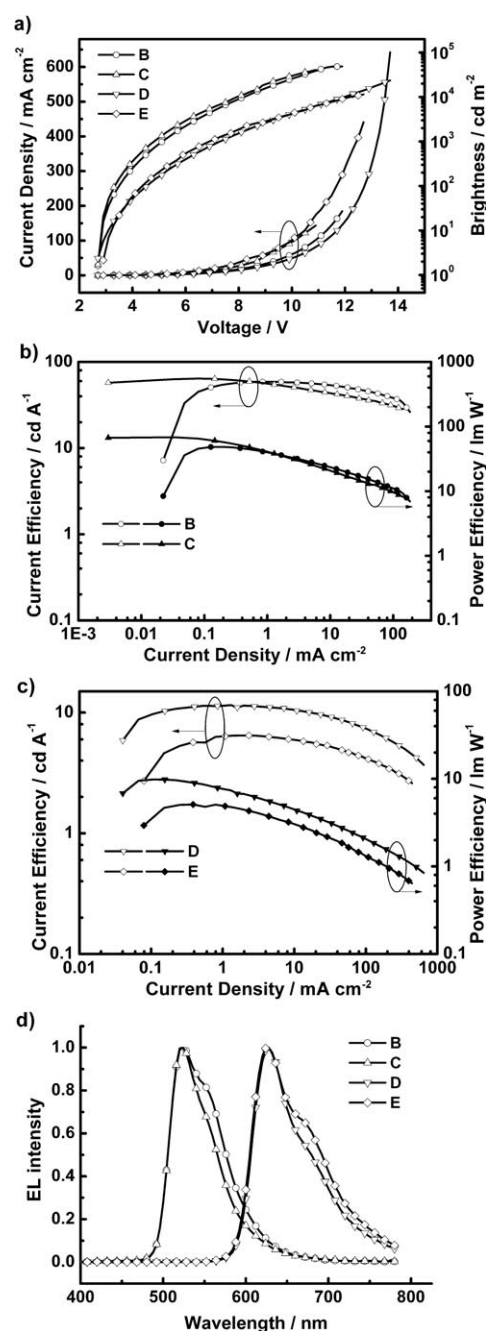


Figure 8. a) Current density–voltage–brightness characteristics for devices **B–E**. b) Current efficiency and power efficiency versus current density curves for devices **B** and **C**. c) Current efficiency and power efficiency versus current density curves for devices **D** and **E**. d) EL spectra for devices **B–E**.

on voltages of 2.7–2.9 V, which could be attributed to their matching HOMO levels (5.2–5.3 eV) with that of the hole-transport NPB layer ($\approx 5.4 \text{ eV}$).

Conclusion

In summary, we have synthesized and characterized two new bipolar molecules that combine triphenylamine and

Table 2. EL performances of devices A–E.

Device ^[a]	EML	$V_{\text{on}}^{\text{[b]}}$ [V]	$L_{\text{max}}^{\text{[c]}}$ [cd m^{-2}] Voltages [V]	$\eta_{\text{c,max}}^{\text{[d]}}$ [cd A^{-1}]	$\eta_{\text{p,max}}^{\text{[e]}}$ [lm W^{-1}]	$\eta_{\text{ext,max}}^{\text{[f]}}$ [%]	CIE ^[g] [x, y]
A	1	3.5	4448, 13.5	2.2	1.6	2.9	0.17, 0.07
B	1-IrG	2.7	48428, 11.9	59.0	48.7	15.5	0.34, 0.62
C	2-IrG	2.7	40702, 10.9	64.3	68.3	17.0	0.32, 0.64
D	1-IrR	2.7	23616, 13.7	11.5	9.8	14.2	0.68, 0.32
E	2-IrR	2.9	11446, 12.7	6.5	5.1	8.3	0.68, 0.32

[a] Devices configuration: ITO/MoO₃ (10 nm)/NPB (80 nm)/EML (20 nm)/TPBI (40 nm)/LiF (1 nm)/Al (100 nm). [b] Turn-on voltages at 1 cd m^{-2} . [c] Maximum luminance. [d] Maximum current efficiency. [e] Maximum power efficiency. [f] Maximum external quantum efficiency. [g] Commission International de l'Éclairage coordinates.

benzimidazole moieties. A nondoped deep-blue fluorescent OLED using **1** as the blue emitter reveals high performance, with a maximum current efficiency of 2.2 cd A^{-1} , and a maximum external efficiency of 2.9% at the CIE coordinates of (0.17, 0.07). Electrophosphorescent devices using the two compounds as host materials for green and red phosphor emitters show high efficiencies. The best performance of the green phosphorescent device was achieved when using **2** as the host, with a maximum current efficiency of 64.3 cd A^{-1} and a maximum power efficiency of 68.3 lm W^{-1} ; whereas the best performance of red phosphorescent device was achieved using **1** as the host, with a maximum current efficiency of 11.5 cd A^{-1} and a maximum power efficiency of 9.8 lm W^{-1} . The results reveal that the bipolar compound **1** has the potential to be a multifunctional material as both deep-blue emitter and host for the phosphorescent dopant in OLEDs.

Experimental Section

General Information

¹H and ¹³C NMR spectra were measured with a MERCURY-VX300 spectrometer. Elemental analyses of carbon, hydrogen, and nitrogen were performed with a Vario EL III microanalyzer. Liquid chromatography (LC) mass spectra were measured with a Waters ZQ-Mass ESI. UV/Vis absorption spectra were recorded with a Shimadzu UV-2500 recording spectrophotometer. Photoluminescence (PL) spectra were recorded with a Hitachi F-4500 fluorescence spectrophotometer. The PL quantum yields were measured from dilute dichloromethane solution (around 10⁻⁶ mol L⁻¹) with the Edinburgh F-900 Instruments integrating sphere excited with an Xe lamp. Differential scanning calorimetry (DSC) was performed with a NETZSCH DSC 200 PC unit at a heating rate of 10 °C min⁻¹ from 30 to 350 °C under argon. The glass-transition temperature (T_g) was determined from the second heating scan. Thermogravimetric analysis (TGA) was undertaken with a NETZSCH STA 449C instrument. The thermal stability of the samples under a nitrogen atmosphere was determined by measuring their weight loss while heating at a rate of 15 °C min⁻¹ from 25 to 600 °C. Cyclic voltammetry (CV) was carried out in nitrogen-purged dichloromethane (oxidation scan) at room temperature with a CHI voltammetric analyzer. Tetrabutylammonium hexafluorophosphate (TBAPF₆) (0.1 M) was used as the supporting electrolyte. The conventional three-electrode configuration consisted of a platinum working electrode, a platinum wire auxiliary electrode, and an Ag wire pseudoreference electrode with ferrocenium–ferrocene (Fc^{+/0}/Fc) as the internal standard. Cyclic voltammograms were obtained at a scan rate of 100 mV s⁻¹. Formal potentials were calculated as the average of cyclic voltammetric anodic and cathodic peaks. The onset potential was determined from the intersection of two tangents drawn at the rising and

background current of the cyclic voltammogram. The starting material 2-(3,5-dibromophenyl)-1-phenyl-1H-benzimidazole (BI-Br₂) was prepared according to the literature procedures.^[25]

Computational Details

The geometric and electronic properties were performed with the Gaussian 03 program package.^[24] The calculation was optimized by means of B3LYP (Becke three-parameter hybrid functional with Lee–Yang–Perdew correlation functionals)^[25] with the 6-31G(d) atomic basis set. Then the electronic structures were calculated at B3LYP/6-311g(d) level. The triplet states $\Delta E (T_1-S_0)$ were calculated using time-dependent density functional theory (TD-DFT) calculations with B3LYP/6-311g(d).

Device Fabrication and Measurement

The hole-injection material MoO₃, hole-transporting material NPB (1,4-bis(1-naphthylphenylamino)biphenyl), and electron-transporting materials 1,3,5-tris(*N*-phenylbenzimidazol-2-yl)benzene (TPBI) were commercially available. Commercial indium tin oxide (ITO)-coated glass with sheet resistance of 10 $\Omega \text{square}^{-1}$ was used as the starting substrate. Before device fabrication, the ITO glass substrates were pre-cleaned carefully and treated by oxygen plasma for 2 min. Then the sample was transferred to the deposition system. MoO₃ (10 nm) was first deposited on the ITO substrate, followed by NPB, the emissive layer, and TPBI (40 nm). Finally, a cathode composed of lithium fluoride (1 nm) and aluminum (100 nm) was sequentially deposited onto the substrate in a vacuum of 10⁻⁶ Torr. The L–V–J of the electroluminescent (EL) devices was measured with a Keithley 2400 Source meter and a Keithley 2000 Source multimeter equipped with a calibrated silicon photodiode. The EL spectra were measured with a JY SPEX CCD3000 spectrometer. All measurements were carried out at room temperature under ambient conditions.

Synthesis of Compound 1

Dry THF (35 mL) was added to a mixture of 2-(3,5-dibromophenyl)-1-phenyl-1H-benzimidazole (0.86 g, 2.00 mmol), 4-(diphenylamino)phenylboronic acid (1.73 g, 6.00 mmol), K₂CO₃ (2 M in H₂O, 6.0 mL, 12.0 mmol), and [Pd(PPh₃)₄] (92 mg, 0.08 mmol). The mixture was heated at reflux for 48 h under argon. After cooling to room temperature, the mixture was poured into water and extracted with CH₂Cl₂. The organic extracts were collected and dried with anhydrous Na₂SO₄. After removal of the solvent, the residue was purified by column chromatography on silica gel using CHCl₃/petroleum (1:1 v/v) as the eluent to give **1** as a white powder. Yield: 56%; m.p.: 256–258 °C; ¹H NMR (300 MHz, CDCl₃): δ = 7.94 (d, J = 7.8 Hz, 1H), 7.74–7.72 (m, 3H), 7.58–7.55 (m, 5H), 7.43–7.40 (m, 5H), 7.30–7.28 (m, 10H), 7.14–7.03 ppm (m, 16H); ¹³C NMR (75 MHz, CDCl₃): δ = 152.28, 147.54, 147.44, 142.94, 141.11, 137.23, 137.14, 134.18, 130.47, 129.99, 129.26, 128.54, 127.78, 127.61, 126.26, 125.87, 124.41, 123.70, 123.40, 122.97, 119.86, 110.42 ppm; MS (ESI): m/z : 757 [$M^+ + 1$]; elemental analysis calcd (%) for C₅₅H₄₀N₄: C 87.27, H 5.33, N 7.40; found: C 87.33, H 4.91, N 7.06.

Synthesis of Compound 2

Compound **2** was prepared according to a similar procedure as **1**. Yield: 62%; m.p.: 211–212 °C; ¹H NMR (300 MHz, CDCl₃): δ = 7.90 (d, J = 7.8 Hz, 1H), 7.64–7.60 (m, 3H), 7.35–7.24 (m, 18H), 7.14–7.09 (m, 12H), 7.04–6.99 ppm (m, 6H); ¹³C NMR (75 MHz, CDCl₃): δ = 152.37, 148.62, 148.16, 143.30, 141.94, 141.83, 137.53, 137.25, 130.92, 130.25, 130.13, 129.66, 129.13, 127.84, 127.61, 127.34, 124.56, 124.28, 123.86, 123.62, 123.43, 123.06, 122.46, 120.27, 110.85 ppm; MS (ESI): m/z : 757 [$M^+ + 1$]; elemental analysis calcd (%) for C₅₅H₄₀N₄: C 87.27, H 5.33, N 7.40; found: C 87.52, H 5.23, N 7.47.

Acknowledgements

We thank the National Natural Science Foundation of China (project nos. 90922020, 50773057, and 20621401) and the National Basic Research Program of China (973 Program; 2009CB623602, 2009CB930603) for financial support.

- [1] a) C. J. Tonzola, A. P. Kulkarni, A. P. Gifford, W. Kaminsky, S. A. Jenekhe, *Adv. Funct. Mater.* **2007**, *17*, 863–874; b) Y. Wei, C.-T. Chen, *J. Am. Chem. Soc.* **2007**, *129*, 7478–7479; c) S. Tao, Y. Zhou, C.-S. Lee, S.-T. Lee, D. Huang, X. Zhang, *J. Phys. Chem. C* **2008**, *112*, 14603–14606; d) Y. Jiang, L. Wang, Y. Zhou, Y.-X. Cui, J. Wang, Y. Cao, J. Pei, *Chem. Asian J.* **2009**, *4*, 548–553.
- [2] a) M.-T. Lee, C.-H. Liao, C.-H. Tsai, C. H. Chen, *Adv. Mater.* **2005**, *17*, 2493–2497; b) S.-L. Lin, L.-H. Chan, R.-H. Lee, M.-Y. Yen, W.-J. Kuo, C.-T. Chen, R.-J. Jeng, *Adv. Mater.* **2008**, *20*, 3947–3952; c) C.-H. Wu, C.-H. Chien, F.-M. Hsu, P.-I. Shih, C.-F. Shu, *J. Mater. Chem.* **2009**, *19*, 1464–1470.
- [3] M.-T. Lee, H.-H. Chen, C.-H. Liao, C.-H. Tsai, C. H. Chen, *Appl. Phys. Lett.* **2004**, *85*, 3301–3303.
- [4] a) M.-Y. Lai, C.-H. Chen, W.-S. Huang, J. T. Lin, T.-H. Ke, L.-Y. Chen, M.-H. Tsai, C.-C. Wu, *Angew. Chem.* **2008**, *120*, 591–595; *Angew. Chem. Int. Ed.* **2008**, *47*, 581–585; b) C.-H. Chen, W.-S. Huang, M.-Y. Lai, W.-C. Tsao, J. T. Lin, Y.-H. Wu, T.-H. Ke, L.-Y. Chen, C.-C. Wu, *Adv. Funct. Mater.* **2009**, *19*, 2661–2670.
- [5] a) C. W. Tang, S. A. VanSlyke, C. H. Chen, *J. Appl. Phys.* **1989**, *65*, 3610–3616; b) C.-G. Zhen, Z.-K. Chen, Q.-D. Liu, Y.-F. Dai, R. Y. C. Shin, S.-Y. Chang, J. Kieffer, *Adv. Mater.* **2009**, *21*, 2425–2429.
- [6] a) Y. Shirota, M. Kinoshita, T. Noda, K. Okumoto, T. Ohara, *J. Am. Chem. Soc.* **2000**, *122*, 11021–11022; b) C.-C. Chi, C.-L. Chiang, S.-W. Liu, H. Yueh, C.-T. Chen, C.-T. Chen, *J. Mater. Chem.* **2009**, *19*, 5561–5571; c) C.-T. Chen, Y. Wei, J.-S. Lin, M. V. R. K. Moturu, W.-S. Chao, Y.-T. Tao, C.-H. Chien, *J. Am. Chem. Soc.* **2006**, *128*, 10992–10993.
- [7] a) C. W. Tang, S. A. VanSlyke, *Appl. Phys. Lett.* **1987**, *51*, 913–915; b) M. A. Baldo, D. F. O'Brien, Y. You, A. Shoustikov, S. Sibley, M. E. Thompson, S. R. Forrest, *Nature* **1998**, *395*, 151–154; c) Y. Sun, N. C. Giebink, H. Kanno, B. Ma, M. E. Thompson, S. R. Forrest, *Nature* **2006**, *440*, 908–912.
- [8] a) Y.-J. Su, H.-L. Huang, C.-L. Li, C.-H. Chien, Y.-T. Tao, P.-T. Chou, S. Datta, R.-S. Liu, *Adv. Mater.* **2003**, *15*, 884–888; b) S.-J. Yeh, M.-F. Wu, C.-T. Chen, Y.-H. Song, Y. Chi, M.-H. Ho, S.-F. Hsu, C. H. Chen, *Adv. Mater.* **2005**, *17*, 285–289; c) N. Rehmman, C. Ulbricht, A. Köhnen, P. Zacharias, M. C. Gather, D. Hertel, E. Holder, K. Meerholz, U. S. Schubert, *Adv. Mater.* **2008**, *20*, 129–133; d) C.-L. Ho, Q. Wang, C.-S. Lam, W.-Y. Wong, D. Ma, L. Wang, Z.-Q. Gao, C.-H. Chen, K.-W. Cheah, Z. Lin, *Chem. Asian J.* **2009**, *4*, 89–103.
- [9] a) W.-Y. Wong, C.-L. Ho, Z.-Q. Gao, B.-X. Mi, C.-H. Chen, K.-W. Cheah, Z. Lin, *Angew. Chem.* **2006**, *118*, 7964–7967; *Angew. Chem. Int. Ed.* **2006**, *45*, 7800–7803; b) C.-L. Ho, W.-Y. Wong, Q. Wang, D. Ma, L. Wang, Z. Lin, *Adv. Funct. Mater.* **2008**, *18*, 928–937; c) G. Zhou, C.-L. Ho, W.-Y. Wong, Q. Wang, D. Ma, L. Wang, Z. Lin, T. B. Marder, A. Beeby, *Adv. Funct. Mater.* **2008**, *18*, 499–511.
- [10] a) Y. Tao, Q. Wang, C. Yang, O. Wang, Z. Zhang, T. Zou, J. Qin, D. Ma, *Angew. Chem.* **2008**, *120*, 8224–8227; *Angew. Chem. Int. Ed.* **2008**, *47*, 8104–8107; b) T.-C. Lee, C.-F. Chang, Y.-C. Chiu, Y. Chi, T.-Y. Chan, Y.-M. Cheng, C.-H. Lai, P.-T. Chou, G.-H. Lee, C.-H. Chien, C.-F. Shu, J. Leonhardt, *Chem. Asian J.* **2009**, *4*, 742–753; c) J.-L. Chen, S.-Y. Chang, Y. Chi, K. Chen, Y.-M. Cheng, C.-W. Lin, G.-H. Lee, P.-T. Chou, C.-H. Wu, P.-I. Shih, C.-F. Shu, *Chem. Asian J.* **2008**, *3*, 2112–2123; d) Y. Tao, L. Ao, Q. Wang, C. Zhong, C. Yang, J. Qin, D. Ma, *Chem. Asian J.* **2010**, *5*, 278–284.
- [11] M. A. Baldo, C. Adachi, S. R. Forrest, *Phys. Rev. B* **2000**, *62*, 10967–10977.
- [12] Y. Tao, Q. Wang, Y. Shang, C. Yang, L. Ao, J. Qin, D. Ma, Z. Shuai, *Chem. Commun.* **2009**, 77–79.
- [13] Y. Q. Li, M. K. Fung, Z. Xie, S.-T. Lee, L.-S. Hung, J. Shi, *Adv. Mater.* **2002**, *14*, 1317–1321.
- [14] a) P.-I. Shih, C.-H. Chien, F.-I. Wu, C.-F. Shu, *Adv. Funct. Mater.* **2007**, *17*, 3514–3520; b) S.-y. Takizawa, V. A. Montes, P. Anzenbacher, Jr., *Chem. Mater.* **2009**, *21*, 2452–2458.
- [15] N. Miyaura, A. Suzuki, *Chem. Rev.* **1995**, *95*, 2457–2483.
- [16] Y. Shirota, *J. Mater. Chem.* **2000**, *10*, 1–25.
- [17] a) Z. Ge, T. Hayakawa, S. Ando, M. Ueda, T. Akiike, H. Miyamoto, T. Kajita, M.-a. Kakimoto, *Adv. Funct. Mater.* **2008**, *18*, 584–590; b) Z. Ge, T. Hayakawa, S. Ando, M. Ueda, T. Akiike, H. Miyamoto, T. Kajita, M.-a. Kakimoto, *Org. Lett.* **2008**, *10*, 421–424.
- [18] W.-Y. Lai, R. Xia, Q.-Y. He, P. A. Levermore, W. Huang, D. D. C. Bradley, *Adv. Mater.* **2009**, *21*, 355–360.
- [19] a) C.-C. Wu, Y.-T. Lin, K.-T. Wong, R.-T. Chen, Y.-Y. Chien, *Adv. Mater.* **2004**, *16*, 61–65; b) J. N. Moorthy, P. Venkatakrishnan, D.-F. Huang, T. J. Chow, *Chem. Commun.* **2008**, 2146–2148; c) Z. Jiang, Z. Liu, C. Yang, C. Zhong, J. Qin, G. Yu, Y. Liu, *Adv. Funct. Mater.* **2009**, *19*, 3987–3995.
- [20] a) Z. Q. Gao, Z. H. Li, P. F. Xia, M. S. Wong, K. W. Cheah, C. H. Chen, *Adv. Funct. Mater.* **2007**, *17*, 3194–3199; b) L. Wang, Y. Jiang, J. Luo, Y. Zhou, J. Zhou, J. Wang, J. Pei, Y. Cao, *Adv. Mater.* **2009**, *21*, 4854–4858; c) C.-H. Chien, C.-K. Chen, F.-M. Hsu, C.-F. Shu, P.-T. Chou, C.-H. Lai, *Adv. Funct. Mater.* **2009**, *19*, 560–566.
- [21] K.-T. Wong, Y.-M. Chen, Y.-T. Lin, H.-C. Su, C.-C. Wu, *Org. Lett.* **2005**, *7*, 5361–5364.
- [22] C.-L. Li, Y.-J. Su, Y.-T. Tao, P.-T. Chou, C.-H. Chien, C.-C. Cheng, R.-S. Liu, *Adv. Funct. Mater.* **2005**, *15*, 387–395.
- [23] Z. Ge, T. Hayakawa, S. Ando, M. Ueda, T. Akiike, H. Miyamoto, T. Kajita, M.-a. Kakimoto, *Chem. Mater.* **2008**, *20*, 2532–2537.
- [24] Gaussian 03, Revision E.01, M. J. Frisch, G. W. Trucks, H. B. Schlegel, G. E. Scuseria, M. A. Robb, J. R. Cheeseman, J. A. Montgomery, Jr., T. Vreven, K. N. Kudin, J. C. Burant, J. M. Millam, S. S. Iyengar, J. Tomasi, V. Barone, B. Mennucci, M. Cossi, G. Scalmani, N. Rega, G. A. Petersson, H. Nakatsuji, M. Hada, M. Ehara, K. Toyota, R. Fukuda, J. Hasegawa, M. Ishida, T. Nakajima, Y. Honda, O. Kitao, H. Nakai, M. Klene, X. Li, J. E. Knox, H. P. Hratchian, J. B. Cross, V. Bakken, C. Adamo, J. Jaramillo, R. Gomperts, R. E. Stratmann, O. Yazyev, A. J. Austin, R. Cammi, C. Pomelli, J. W. Ochterski, P. Y. Ayala, K. Morokuma, G. A. Voth, P. Salvador, J. J. Dannenberg, V. G. Zakrzewski, S. Dapprich, A. D. Daniels, M. C. Strain, O. Farkas, D. K. Malick, A. D. Rabuck, K. Raghavachari, J. B. Foresman, J. V. Ortiz, Q. Cui, A. G. Baboul, S. Clifford, J. Cioslowski, B. B. Stefanov, G. Liu, A. Liashenko, P. Piskorz, I. Komaromi, R. L. Martin, D. J. Fox, T. Keith, M. A. Al-Laham, C. Y. Peng, A. Nanayakkara, M. Challacombe, P. M. W. Gill, B. Johnson, W. Chen, M. W. Wong, C. Gonzalez, J. A. Pople, Gaussian, Inc., Wallingford CT, **2004**.
- [25] a) A. D. Becke, *Phys. Rev. A* **1988**, *38*, 3098–3100; b) C. Lee, W. Yang, R. G. Parr, *Phys. Rev. B* **1988**, *37*, 785–789.

Received: March 16, 2010
 Published online: July 22, 2010